Valence state of Ti in conductive nanowires in sapphire

Teruyasu Mizoguchi,[1] Masaki Sakurai,[2] Atsutomo Nakamura,[1] Katsuyuki Matsunaga,[1,*] Isao Tanaka,[3] Takahisa Yamamoto,[4] and Yuichi Ikuhara[1]

[1]*Institute of Engineering Innovation, The University of Tokyo, 2-11-6, Yayoi, Bunkyo, Tokyo 113-8656, Japan*

[2]*Institute for Materials Research, Tohoku University, Katahira 2-1-1, Aoba, Sendai 980-77, Japan*

[3]*Department of Materials Science and Engineering, Kyoto University, Yoshida, Sakyo, Kyoto 606-8501, Japan*

[4]*Department of Advanced Materials Science, Graduate School of Frontier Science, The University of Tokyo, 2-11-16, Yayoi, Bunkyo, Tokyo 113-8656, Japan*

(Received 29 January 2004; revised manuscript received 14 May 2004; published 5 October 2004)

In order to reveal the valence state of Ti in conductive nanowires in sapphire, near-edge x-ray-absorption fine structures (NEXAFS) were observed. From experimental and theoretical studies on NEXAFS of reference compounds including rutile, anatase, and Ti_2O_3, it was found that the valence state of Ti can be identified by regarding the positions of the spectral onset and the shoulder in the main peak of Ti-K NEXAFS. The valence states of Ti doped Al_2O_3 polycrystalline specimens which were annealed at oxidized and reduced atmospheres were determined to be +4 and +3, respectively. The solubility limit of Ti in Al_2O_3 polycrystal was found to be between 1000 ppm to 1.0% at the both atmospheres. The spectrum from Ti nanowires in sapphire has a lot of similarities to the reduced specimen, the valence state was therefore concluded to be +3.

DOI: 10.1103/PhysRevB.70.153101 PACS number(s): 61.72.−y, 73.90.+f, 61.10.Ht

Al_2O_3 is well known to maintain high mechanical strength, toughness, and corrosion resistance up to high temperature, which are advantageous for the applications as the high-temperature structural material.[1,2] Mechanical properties of Al_2O_3 are affected by the grain boundaries, and thus a number of recent studies on Al_2O_3 have focused on atomic structures of the grain boundaries.[3–5] On the other hand, for electric application, Al_2O_3 is commonly used as insulator due to the high electric conductivity of around $<1\times10^{-14}\ \Omega^{-1}\ cm^{-1}$. Recently, Nakamura *et al.* succeeded in doping Ti along unidirectional dislocations in Al_2O_3 single crystal (sapphire), and the electric conductivity of $1\times10^{-1}\ \Omega^{-1}\ cm^{-1}$ along the Ti-enriched dislocations was attained.[6] Therefore, it can be said that Ti from one-dimensional conductive nanowires in sapphire. Such a doping technique to dislocations has a potential to give unusual physical properties to commonly used materials.

In case of the Ti nanowires in sapphire, electronic structures of Ti may play an important role for the electric conductivity. Ti can have various valence states such as Ti^{2+}, Ti^{3+}, and Ti^{4+}. Thus the valence state of Ti in the nanowires and its relation to macroscopic properties are interesting to be investigated. The aim of this study is identification of the valence state of Ti at the nanowires using near-edge x-ray-absorption fine structures (NEXAFS). NEXAFS reflects an electron transition from a core orbital to unoccupied bands. The spectral onset and features provide us information on the valence state and local electronic structures of an objective atom.

In this work, Ti-K NEXAFS were observed at BL12C in Photon Factory, KEK, Japan.[7,8] Si(111) double crystals were employed as a monochromator. Fluorescence from samples was collected by 19-elements Ge solid-states detector. Using such a high sensitivity detector, NEXAFS from dilute dopant of a ppm-order can be observed with sufficient signal to noise ratio.[9] Ti nanowires were fabricated in sapphire in the manner described in Ref. 6. Unidirectional dislocations were introduced along the direction of $[1\bar{1}00]$ of sapphire by high-temperature plastic deformation. Ti metals were deposited on the deformed specimen, and postannealing was performed at 1773 K in $Ar+5\%H_2$ for 12 h so as to infiltrate Ti atoms along the dislocation. Figure 1 shows the bright field TEM image of the unidirectional dislocations fabricated by the above procedure. In order to clearly observe the unidirectional dislocations, the TEM image was obtained for the specimen tilted around $[11\bar{2}0]$ axis from the edge-on $[1\bar{1}00]$ direction.

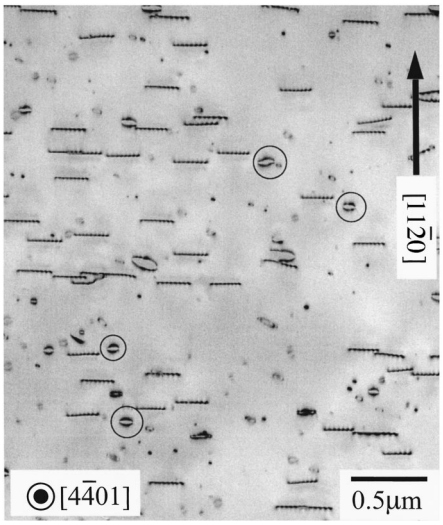

FIG. 1. Bright field TEM image of the unidirectional dislocations which are arrayed along the direction of $[1\bar{1}00]$. The TEM image is obtained from the specimen tilted around $[11\bar{2}0]$ axis to $[44\bar{0}1]$ zone. Some of loop dislocations are also observed e. g., surrounding areas by circles.

It is clearly found that the dislocations are arrayed, and completely penetrated through the specimen. By using the nanoprobe TEM-EDS (EDSI energy dispersive spectrascopy) technique, it was found that the Ti are localized around the dislocations within 5 nm diameter, and the concentration of Ti in the vicinity of a nanowire is about 18 at %.[6] The total concentration of Ti in the specimen is estimated to be 100 ppm. For comparision, 200 ppm Ti-doped sapphire was also prepared, and it was postannealed with the same condition as that for the Ti nanowires. As reference samples, Ti-doped Al_2O_3 polycrystals were fabricated with the concentration between 100 ppm to 1 at %. Sintering was perfromed in air at 1673 K for 4 h. In order to confirm the effect of atmosphere at the postannealing on the valence state of Ti, annealing both at oxidized (oxygen) and reduced ($Ar+5\%H_2$) atmospheres were individually made at 1623 K for 12 h after the sintering.

In order to understand the spectral features depending on the valence state of Ti, NEXAFS of Ti oxides were examined. Figure 2 shows Ti-K NEXAFS of TiO_2 (rutile), TiO_2 (anatase), and Ti_2O_3 (corundum structure) observed in the present study. Formal charges of Ti in the former two oxides are +4, whereas that in Ti_2O_3 is +3. The Ti-K NEXAFS can be divided into two parts, one is a set of small peaks within 8 eV from spectral onsets, and the other is that of the following large peaks. They are hereafter called "prepeak" and "mainpeak" for simplicity. Although the spectral features of the Ti^{4+} compounds are slightly different from each other, the following two characteristics are commonly found. (1) The onset of the prepeak is 4953 eV. (2) The shoulder is found at 496 eV in the main peak. On the other hand, the onset of the prepeak and the shoulder in the main peak appear at 4951 eV and 4962 eV in the spectrum of Ti_2O_3. In order to ensure the spectral differences between the Ti^{4+} and Ti^{3+} oxides, theoretical calculations of NEXAFS have been performed by the first-principles band-structure calculation using the orthogonalized linear combinations of atomic orbitals (OLCAO) method.[10] A core-hole which is accompanied with an electron transition was fully taken account at the final state calculation. Both ground and final states were separately calculated, and the difference of the total energy was employed as a theoretical transition energy. In order to minimize interactions among the core-holed atoms in adjacent cells, 72, 108, and 120 atoms supercells were employed for rutile, anatase, and Ti_2O_3, respectively. It has been proved that the OLCAO calculation with the core-hole effect well reproduces the experimental NEXAFS.[9–16] Although the onsets of the calculated spectra were shifted by +8 eV, it should be noted that the calculation error is 0.2% of the absolute transition energy. The above spectral differences between the Ti^{4+} and Ti^{3+} oxides in experiments were well reproduced by the theoretical calculations. Therefore, the valence state of Ti in Al_2O_3 can also be identified from the energy positions of the onset of the pre peak and the shoulder in the main peak.

Figure 3 shows a series of Ti-K NEXAFS from Ti doped Al_2O_3 polycrystals after the heat treatments in the oxidized and reduced atmospheres together with the spectrum of Al_2TiO_5. In the both heat treated specimens, the spectral features do not change up to the concentration of 1000 ppm. On the other hand, the spectra of 1% Ti doped specimens exhibits a distinctive peak at 4973 eV indicated by the upward arrow, which corresponds to the main peak of Al_2TiO_5. This indicates that the solubility limit of Ti in Al_2O_3 at both atmospheres is between 1000 ppm to 1%. The solubility limits of Ti in Al_2O_3 at reduced and oxidized atmosphere have been reported to be 1% at 1673 K (Ref. 17) and 3000 ppm at 1573 K,[18] respectively. In addition, the solution energy of Ti to Al_2O_3 was recently evaluated by the first-principles plane-wave basis pseudoptential calculation.[19] The theoretical study predicted the same solubility limit of Ti at both atmospheres. The obtained value in this study is within the range of the previous experimental results, and is consistent to the theoretical prediction.

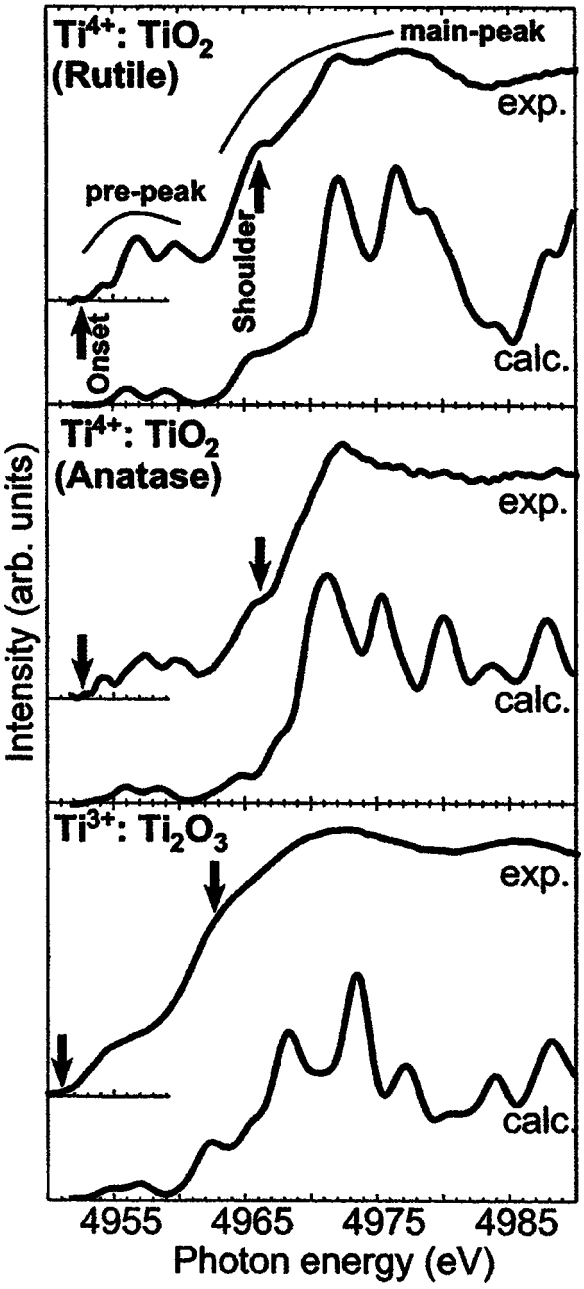

FIG. 2. (Top to bottom) Experimental and theoretical Ti-K NEXAFS of TiO_2 (rutile), TiO_2 (anatase), and Ti_2O_3.

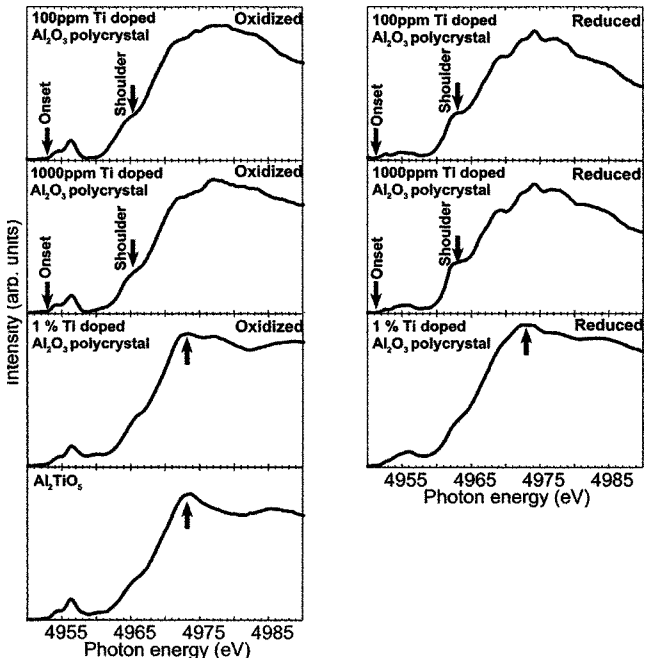

FIG. 3. A series of Ti-K NEXAFS from Ti-doped Al_2O_3 polycrystalline specimens after annealing at the oxidized atmosphere (left) and at the reduced atmosphere (right). The concentration of Ti is from 100 ppm to 1%. The bottom spectrum of the left column is measured from Al_2TiO_5 powder.

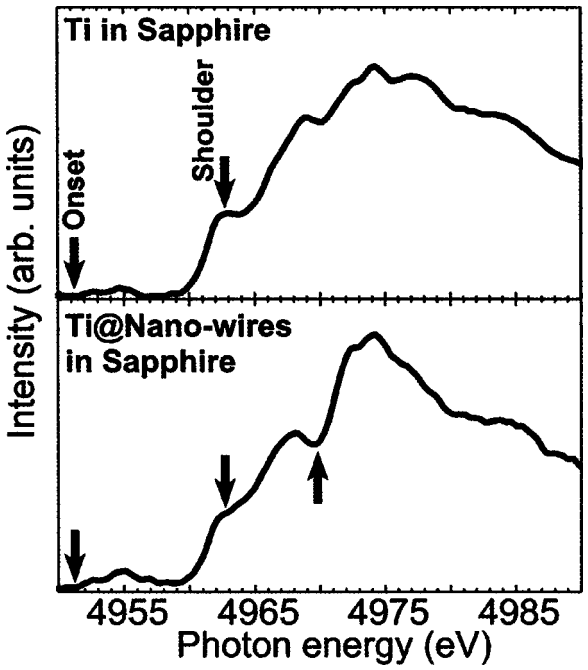

FIG. 4. Ti-K NEXAFS from Ti doped sapphire (top) and that from Ti nanowires in sapphire (bottom).

The spectra from the less than 1000 ppm Ti doped specimens are apparently different from those of reference compounds in Fig. 2. In addition, it is clearly found that the spectral features change with the heat treatment atmospheres. As compared to oxidized specimens, the positions of the onset of the prepeak and the shoulder in the main peak are located at 2–4 eV lower-energy side in the reduced specimens. The spectral differences are the same as that for the Ti^{4+} and Ti^{3+} oxides shown in Fig. 2. Therefore, it can be concluded that Ti in the oxidized polycrystaline Al_2O_3 are close to +4, while +3 in the reduced polycrystalline Al_2O_3.

NEXAFS from Ti-doped sapphire and Ti nanowires were shown in Fig. 4. The spectrum of the Ti-doped sapphire is almost indentical to that of the reduced polycrystalline specimen with the concentration of 100 ppm shown in Fig. 3. The valence state of Ti dissolved in sapphire can be thus determined to be +3, which is consistent with the previous literature.[20] In the case of the spectrum from the Ti nanowires, although the characteristic concave feature is found at 4971 eV, the main features have a lot of similarities to those of Ti-doped sapphire. In addition, the onset of the prepeak and the shoulder in the main peak are located at 4951 and 4962 eV. Therefore, the valence state of Ti in the conductive nanowires in sapphire is concluded to be +3.

These results indicate that the Ti 3*d* bands in the nanowire, which are formed between the band gap,[21] are partially occupied because an isolated Ti^{3+} ion has one electron at the 3*d* orbital. It should be recalled that the solubility limit of the Ti^{3+} ion in the polycrystalline Al_2O_3 is less than 1%. In contrast, the Ti^{3+} ion of the nanowires were forced to be localized and concentrated around the dislocations with the concentration of $\sim$18%.[6] Such highly concentrated state should be caused by the unusual atomic and electronic structures of the dislocations. Recently, association of the Ti^{3+} ions in Al_2O_3 was predicted by the first-principle plane-wave basis pseudoptential calculation.[21] Although the calculation was made for the Ti in the bulk Al_2O_3, it is expected that the tendency is emphasized in the dislocations due to the unusual environments. Both of the partially occupied Ti-3*d* bands and the highly concentrated Ti^{3+} in the nanowires are considered to play an important role to bring about the electric conductivity.

We thank Professor W. Y. Ching at the University of Missouri-Kansas City for allowing us to use the OLCAO code. T.M. appreciates Dr. T. Yamamoto and Dr. T. Suga for their helpful discussion. T.M. also thanks M. Kunisu, S. Yoshioka, N.Yamada, and S. Kameyama for their help in measuring NEXAFS. T.M. and A.N. are supported as JSPS research fellows. This work was supported by a Grant-in-Aid for Scientific Research and Special Coordination Funds from the Ministry of Education, Culture, Sports, Science and Technology of the Japanese government.

*Author to whom correspondence should be addressed; Email address: matu@sigma.t.u-tokyo.ac.jp

[1] R. M. Cannon, W. H. Rhodes, and A. H. Heuer, J. Am. Ceram. Soc. **63**, 46 (1980).
[2] H. Yoshida, Y. Ikuhara, and T. Sakuma, Acta Mater. **50**, 2955 (2002).
[3] Y. Ikuhara, H. Nishimura, A. Nakamura, K. Matsunaga, and T. Yamamoto, J. Am. Ceram. Soc. **86**, 595 (2003).
[4] H. Nishimura, K. Matsunaga, T. Saito, T. Yamamoto, and Y. Ikuhara, J. Am. Ceram. Soc. **86**, 574 (2003).
[5] K. Matsunaga, H. Nishimura, H. Muto, T. Yamamoto, and Y. Ikuhara, Appl. Phys. Lett. **82**, 1179 (2003).
[6] A. Nakamura, K. Matsunaga, J. Tohma, T. Yamamoto, and Y. Ikuhara, Nat. Mater. **2**, 453 (2003).
[7] M. Nomura and A. Koyama, J. Synchrotron Radiat. **6**, 182 (1999).
[8] M. Nomura and A. Koyama, Nucl. Instrum. Methods Phys. Res. A **467–468**, 733 (2001).
[9] I. Tanaka, T. Mizoguchi, M. Matsui, S. Yoshioka, H. Adachi, T. Yamamoto, T. Okajima, M. Umesaki, W. Y. Ching, Y. Inoue, M. Mizuno, H. Araki, and Y. Shirai, Nat. Mater. **2**, 541 (2003).
[10] W. Y. Ching, J. Am. Ceram. Soc. **73**, 3135 (1990).
[11] S. D. Mo and W. Y. Ching, Phys. Rev. B **62**, 7901 (2000).
[12] T. Mizoguchi, I. Tanaka, S. Yoshioka, M. Kunisu, T. Yamamoto, and W. Y. Ching, Phys. Rev. B **70**, 045103 (2004).
[13] T. Mizoguchi, I. Tanaka, M. Kunisu, M. Yoshiya, H. Adachi, and W. Y. Ching, Micron **34**, 249 (2003).
[14] W. Y. Ching, S. D. Mo, and Y. Chen, J. Am. Ceram. Soc. **85**, 11 (2002).
[15] Y. N. Xu, Y. Chen, S. D. Mo, and W. Y. Ching, Phys. Rev. B **65**, 235105 (2002).
[16] S. D. Mo and W. Y. Ching, Appl. Phys. Lett. **78**, 3809 (2001).
[17] W. D. Mckee, Jr. and E. Aleshin, J. Am. Ceram. Soc. **46**, 54 (1963).
[18] E. R. Winkler, J. F. Sarver, and I. B. Cutler, J. Am. Ceram. Soc. **49**, 634 (1966).
[19] K. Matsunaga, A. Nakamura, T. Yamamoto, and Y. Ikuhara, Phys. Rev. B **68**, 214102 (2003).
[20] K. Eigenmann and H. H. Günthard, Chem. Phys. Lett. **13**, 58 (1972).
[21] K. Matsunaga, T. Mizoguchi, A. Nakamura, T. Yamamoto, and Y. Ikuhara, Appl. Phys. Lett. **84**, 4795 (2004).